

# Optimal Sizing of Behind-the-Meter Battery Storage for Providing Profit-Oriented Stackable Services

Yichao Zhang<sup>ID</sup>, Graduate Student Member, IEEE, Amjad Anvari-Moghaddam<sup>ID</sup>, Senior Member, IEEE, Saeed Peyghami<sup>ID</sup>, Senior Member, IEEE, Yuan Li<sup>ID</sup>, Graduate Student Member, IEEE, Tomislav Dragičević<sup>ID</sup>, Senior Member, IEEE, and Frede Blaabjerg<sup>ID</sup>, Fellow, IEEE

**Abstract**—This paper focuses on an advanced optimization method for optimizing the size of the behind-the-meter (BTM) battery energy storage system (BESS) that provides stackable services to improve return on investment. The grid frequency regulation service and two customer-side services, i.e., energy arbitrage and peak shaving, are selected as stackable services of BTM BESS. A two-stage stochastic programming model is proposed to handle uncertainty and achieve the most cost-effective BTM BESS size. The first stage obtains the optimal BTM BESS size with the maximum annual net income. The operating strategy of the BTM BESS is optimized in the second stage to maximize revenue while considering the BTM BESS degradation cost and the uncertainty of operating scenarios. A hybrid solution algorithm combining genetic algorithm and mixed-integer linear programming is employed to solve the two-stage stochastic programming model. A strategy based on a recorder and a filter is proposed to speed up the solution. In addition, a novel method for converting the second-level regulation signal into the equivalent minute-level signal is offered to reduce computational burden while maintaining high accuracy. Finally, the effectiveness of the proposed method is validated based on an industrial load and regulation information from the Pennsylvania-New Jersey-Maryland (PJM) market.

**Index Terms**—Sizing optimization, BTM BESS, stackable services, equivalent regulation signal, hybrid algorithm, peak shaving, energy arbitrage, frequency regulation.

## NOMENCLATURE

The main notation of this paper is stated as follows. The superscripts are utilized to distinguish and illustrate the parameters and variables. The subscripts are indexed to denote the time and scenario.

## Acronym

BTM	Behind-the-meter
BESS	Battery energy storage system
MILP	Mixed-integer linear programming

Manuscript received 30 December 2022; revised 6 May 2023; accepted 18 June 2023. Date of publication 10 July 2023; date of current version 21 February 2024. This work was supported by the China Scholarship Council (CSC). Paper no. TSG-01956-2022. (Corresponding author: Yichao Zhang.)

Yichao Zhang, Amjad Anvari-Moghaddam, Saeed Peyghami, Yuan Li, and Frede Blaabjerg are with the AAU Energy, Aalborg University, 9200 Aalborg, Denmark (e-mail: yzha@energy.aau.dk; aam@energy.aau.dk; sap@energy.aau.dk; yuanli@energy.aau.dk; fbl@energy.aau.dk).

Tomislav Dragičević is with the DTU Wind and Energy Systems, Technical University of Denmark, 2800 Lyngby, Denmark (e-mail: tomdr@dtu.dk).

Color versions of one or more figures in this article are available at <https://doi.org/10.1109/TSG.2023.3292076>.

Digital Object Identifier 10.1109/TSG.2023.3292076

EA	Energy arbitrage
PS	Peak shaving
FR	Frequency regulation
SoC	State of charge

## Indices and Sets

$t$	Index of time interval of optimization model
$t_1$	Index of time interval of FR signal
$h$	Index of hour in a day
$d$	Index of day in a month
$m$	Index of month in a year
$l$	Index of typical scenarios

## Parameters

$\Delta t, \Delta t_1$	Duration of each time interval of $t, t_1$
$\Delta t_2$	Resolution of load profiles
$T, T_1$	Number of time intervals $t, t_1$ in an hour
$H$	Number of hours in a day
$D_m$	Number of days in month $m$
$M$	Number of months in a year
$L$	Number of typical operating scenarios
$\sigma_{t,h,d}^{EA}, \sigma_{t,h,d}^{PS}$	Energy price and demand charge price, \$/kWh, \$/kW
$\sigma_h^{FR}$	Hourly regulation price, \$/kWh
$C_{Bgt}^{Bgt}$	BESS investment budget limitation, \$
$\sigma^E, \sigma^P$	BESS cost of per kWh and per kW, \$/kWh, \$/kW
$\eta^c, \eta^d$	Charge and discharge efficiency of BESS, %
$r$	Interest rate, %
$N$	Project planning time, years
$SoC^{lb}, SoC^{ub}$	Lower and upper bound of SoC, %
$SoC^{ini}$	Initial SoC of BESS, %
$f_{t,h}, f_{t,h}^+, f_{t,h}^-$	FR signal, positive and negative FR signal
$P_{t,h,d}^{load}$	Customer load, kW
$P_{t,h,d}^{PD}$	Original peak demand in a billing period, kW
$E^{lb}, E^{ub}$	Lower and upper bounds of BESS energy size, kWh
$P^{lb}, P^{ub}$	Lower and upper bounds of BESS power size, kW
$N^{cycle}$	Cycle numbers of BESS in $[SoC^{lb}, SoC^{ub}]$
$X, X_b$	Decimal format and binary format of a decision variable
$X^{\min}, X^{\max}$	Designed solution space of $X$
$N_b$	Number of bits in the binary string $X_b$

$p(l)$	Probability of the scenario $l$ , %
$\Delta SoC_{\Delta t_1, \Delta t}$	Variation of $SoC$ during $\Delta t$ based on the signal with the resolution of $\Delta t_1$

### Continuous Variables

$B, B^{BE}$	Electricity bill without and with BESS, \$
$R^{EM}, R^{FR}$	Revenue of energy management and FR, \$
$R_m$	Monthly net revenue of stackable services, \$
$P^{PD,BE}$	Peak demand with BESS in a billing period, kW
$ANI$	Annual net income of BESS, \$
$C^{inv}$	Annual investment cost of BESS, \$
$C^{O&M}$	Operation and management cost of BESS, \$
$C^{de}$	Degradation cost of BESS, \$
$P_{t,h,d}$	Power exchange of BESS, kW
$P_{t,h,l}^{EM}, P_{t,h,l}^{FR}$	BESS power for EA and PS, FR, kW
$P_{t,h,l}^d, P_{t,h,l}^c$	BESS discharge and charge power, kW
$P_{thr}$	Threshold for peak shaving, kW
$\delta_h$	Hourly FR performance score, %
$C_h^{bid}$	Hourly regulation capacity, kW

### Discrete variables

$E^{rate}, P^{rate}$	BESS rated energy and power size, kWh, kW
----------------------	---

### Binary variable

$s_h$	Decision on whether BESS offers FR in $h$ hour
-------	--

## I. INTRODUCTION

**B**EHIND the meter (BTM) battery energy storage system (BESS) is often referred to as small-scale stationary batteries, which are usually connected to behind the utility meter of residential, commercial, and industrial customers in the distribution network [1]. BTM BESS can provide a range of services to satisfy customer requirements, as well as additional services to support the grid [2]. Due to the financial barrier, the adoption of BTM BESS among industrial customers is not widespread [3]. Although BESS prices have experienced a steep decline from 2010 to 2020 [4], the upfront cost of large-size BTM BESS is still prohibitively expensive for industrial customers with heavy loads. Achieve the profit-oriented BESS investment by selecting suitable services and optimizing the size is an effective way to promote the deployment of BTM BESS by industrial customers.

Electricity bill saving is a key factor in attracting industrial customers when the investment of BTM BESS is profit oriented. The bill reduction is primarily achieved by energy management services, i.e., energy arbitrage and peak shaving. The former service shifts load from high-cost periods to low-cost periods, while the latter reduces peak electricity usage during billing periods. However, relying on customer-side services only hardly offsets the investment cost or has a slow payback rate [5]. Apart from customer-side services, providing grid ancillary services can bring additional revenue to owners. Among grid ancillary services, the frequency regulation service is regarded as the most lucrative choice [6]. The BESS is the most competitive candidate to provide frequency regulation service due to its fast and accurate response. The synergy

between frequency regulation and customer-side services is expected to make the BTM BESS fully utilized and realize higher revenue. The economic and technical feasibility of BESS providing stackable services to improve profitability is proved in [7], [8], [9] by conducting the tech-economic analysis or cost-economic assessment. Therefore, considering stackable services consisting of both customer-side services and grid services in the planning of BTM BESS is a promising way to improve the profitability.

### A. Literature Survey

Extensive research has been conducted for the sizing optimization of BESS considering only one service, such as energy arbitrage [10], peak shaving [11], frequency regulation [12], and reliability [13], etc. A few studies have incorporated stackable revenues in the planning of BESSs [14], [15], [16]. A multi-objective approach is employed in [14] to size BESS, which provides peak shaving and frequency regulation service. A bi-level ESS planning method considering comprehensive benefits is presented in [15], where the stackable revenue includes energy arbitrage, reserve benefit, and carbon emission reduction benefit. The economic revenue from peak shaving, frequency regulation, and upgrade deferral of a system of shared energy storage (SES) are considered in [16]. However, these works are mainly for grid-connected BESS.

Different from the grid-connected BESS, the BTM BESS is managed by the independent customer instead of the grid. In recent years, the BTM BESS has been applied to different application scenarios including improving self-consumption by combining with renewable energy [17], reducing electricity bills by participating in demand response [18], and enhancing resiliency during grid outages [19]. Despite the great beneficial effects, the BTM BESS owners must be careful when choosing the capacity due to the large upfront investment cost.

Research on the capacity planning of BTM BESS usually focuses on a single type of customer-side service. The battery sizing of the household system is optimized in [20] to increase the value of self-consumption. A framework for designing the battery capacity is presented in [21] for enhancing the resilience of an airport. Since the revenue from a single service is difficult to attract sufficient investment interest, some research has attempted to consider multiple services in the capacity planning of BTM BESS. A bi-level optimization model is developed for industrial customers to determine the size of BESS, which considers both energy arbitrage and peak demand management of the BESS [22]. Considering the on-and off-grid operation of a hybrid energy system with a battery, the sizing of the battery is optimized, which takes into the benefits from energy arbitrage, peak demand charge, and reliability [23]. However, the stackable services in [22], [23] are combinations of customer-side services. Currently, few studies consider the combination of customer-side services with frequency regulation in the BTM BESS planning process. The reason behind this is that some BTM BESSs only require a small capacity [17], [18], [20], [22], which cannot reach the lowest threshold for participating in the regulation market. In contrast, the BTM BESS invested by industrial customers has a larger capacity, making it possible to participate in frequency

regulation services. To fill this gap, this paper aims to address the BTM BESS capacity planning problem considering the synergy of customer-side services and the grid-side frequency regulation service.

Both the modeling and solution methods are essential for the BTM BESS capacity planning. There are several challenges for this modeling. Firstly, the revenue model of frequency regulation service is complex, which involves the regulation capacity submission by customers and the performance of BESS following the frequency signal. Reference [7] adopted a penalty price to represent the regulation performance, while the model is not accurate when the bidding capacity is zero. The performance is simplified as 1 to neglect its influence in [24], [25], [26]. In [27], the submitted frequency regulation capacity is taken as a constant instead of a variable in the co-optimization of energy arbitrage and frequency regulation, which may lead to a suboptimal solution. Secondly, the three services have different resolutions and billing periods, which results in difficulties in the synergy of the three services. The energy arbitrage is conducted for one day with a time resolution of an hour. Peak shaving benefits are usually calculated based on the highest electricity usage lasting 15 minutes during a billing period. The BESS responds to regulation signals with a resolution of 2 seconds during an hour horizon. Therefore, the operating strategy of a BESS for providing the three stackable services should be optimized with a time step of 2 seconds based on all operating scenarios during a billing period. Obviously, it is intractable directly. In order to enhance computational efficiency, current research extends the original frequency sampling time to different levels. For instance, the sampling time is directly extended to 10 seconds [27], 15 minutes [24], [25], [26], and 1 hour [8], respectively. In contrast, [13] and [28] take the average value of frequency signals as the sampling value of the enlarged interval. However, such sampling methods will change daily regulation signal scenarios and introduce large errors into the model thus misleading investors. In [29], three stackable services are co-optimized based on a dynamic programming model, where both the frequency bidding capacity and regulation performance are considered. However, applying the real-time operating strategy at the planning stage is complicated due to the large computational burden.

The challenge in terms of solution originates from co-optimizing the BESS size and operating strategy. In the previous research, the two-stage programming model or bi-level optimization model is usually employed [10], [15], [16], [30], [31], [32] to consider the inherent correlation between size and operating strategy. However, these models often involve a large-scale optimization problem with non-linear terms, which makes it challenging to find an exact solution in an acceptable time. Mathematical methods [10], heuristics methods [33], [34], [35], and their combinations [16], [28], [36] have been developed to tackle these models. A two-stage stochastic bi-level programming model is presented in [10] to best allocate BESS in the distribution network for arbitrage. Mathematical methods, such as the Karush-Kuhn-Tucker optimality conditions, strong duality theory, and the big-M method, are utilized to transform the bi-level model into

a tractable mixed-integer linear programming (MILP) model. The mathematical method can derive an exact solution, but it requires intricate mathematical transformations and a notable convergence time. To overcome the above drawbacks, heuristic methods, such as genetic algorithm (GA) [33], [37], and particle swarm optimization [34], [35], are developed. The nested GA is utilized to solve the SES bi-level planning model [16], where GA determines the SES size in the upper-level model, and the day-ahead dispatch strategies are also optimized by GA in the lower-level model. Although heuristic methods can effectively reduce computational burdens, converging to the local optimum is possible. Running the heuristic algorithm multiple times is a recommended practice to search for the best solution [33], [35]. However, repeated solutions generated in the single run and multiple runs of the heuristic algorithm induce redundant calculations for their objective function. Furthermore, the size of BESS for supporting the fast-charging station is optimized in [36], where a GA-MILP hybrid algorithm is utilized to solve the bi-level model with non-linear terms. The BESS sizing is searched by GA and as input of the MILP model for optimizing the fast-charging station operation. This method reduces the calculational complexity by avoiding dealing with the non-linear term by mathematic methods.

## B. Contributions

Compared to our previous work [28], three stackable services are considered in this paper for further improving the profitability of BTM BESS. The newly introduced service-peak shaving amplifies the complexity and scale of the BESS sizing optimization problem, which requires efforts to strike a balance between the solution accuracy and efficiency. The main contributions of this paper are summarized as follows:

1) A two-stage stochastic programming framework is established for ascertaining the most cost-effective size of BESS, which offers three stackable services. The framework takes into account the uncertainty of operating scenarios and the BESS degradation cost, which facilitates the investors to make a robust and informed decision.

2) A method is proposed to equivalently convert the original second-level frequency regulation signal into the minute-level one. The equivalent regulation scenarios with required resolution will be used as the input of the BESS operating model, targeting to reduce the computational burden while keeping the effectiveness of regulation results.

3) Since the proposed two-stage stochastic programming framework is a large-scale mixed-integer non-linear programming (MINLP) problem, the GA-MILP hybrid algorithm is employed to solve it. A strategy based on a filter and a recorder is proposed to speed up the solution.

The remaining part of the paper is organized as follows. Section II presents the market rules for the provided three services. Section III introduces the two-stage stochastic programming framework for co-optimizing BESS sizing and operating strategy. Section IV illustrates the generation of typical operating scenarios with an associated probability. Besides, a model for generating an equivalent regulation signal with the required resolution is presented in this section. The method

for solving the two-stage stochastic programming framework is demonstrated in Section V. A numerical analysis is shown in Section VI followed by conclusions in Section VII.

## II. MARKET FRAMEWORK

Market framework and price mechanism have significant influence on the BEES investment [38]. This section introduces the market rules and revenue models of energy arbitrage, peak shaving, and frequency regulation that are adopted in this work.

### A. Energy Arbitrage and Peak Shaving

Large electricity consuming customers are usually billed for energy in two ways: energy charge and peak demand charge. The energy charge is related to electricity consumed. The peak demand charge depends on the average value of the highest electricity consumption over a defined time interval (usually 15 min) during a billing period (usually 1 month). The electricity bill for a large electricity customer without BESS during a billing period is calculated as (1).

$$B = \sigma^{PS} P^{PD} + \sum_{d=1}^D \sum_{h=1}^H \sum_{t=1}^T \sigma_{t,h,d}^{EA} P_{t,h,d}^{load} \Delta t \quad (1)$$

When a BESS is installed for reducing electricity bills, its bill  $B^{BE}$ , and the revenue  $R^{EM}$  which is equal to the saved bill can be calculated as (2) and (3).

$$B^{BE} = \sigma^{PS} P^{PD,BE} + \sum_{d=1}^D \sum_{h=1}^H \sum_{t=1}^T \sigma_{t,h,d}^{EA} (P_{t,h,d}^{load} - P_{t,h,d}) \Delta t \quad (2)$$

$$R^{EM} = B - B^{BE} = \sigma^{PS} (P^{PD} - P^{PD,BE}) + \sum_{d=1}^D \sum_{h=1}^H \sum_{t=1}^T \sigma_{t,h,d}^{EA} P_{t,h,d} \Delta t \quad (3)$$

### B. Frequency Regulation Revenue

The extra revenue can be generated from offering frequency regulation. At present, multiple independent system operators (ISOs) have allowed customer-side BESS to provide frequency regulation. Also, mature market mechanisms have been formulated to pay for this service. Here, the policy from Pennsylvania-New Jersey-Maryland (PJM) market is adopted as an example to establish the regulation revenue model.

The BESS operator is required to determine regulating hours of the next day and submit the bidding capacity in advance. During operating hours, the BESS resources will respond to the real-time regulating signal (RegD), which is sent to the individual resources every 2 seconds. After the operating hour, PJM will compute the regulation performance score, and clear the hourly revenue based on the performance score and the bidding capacity. Notice, the lowest limit for bidding capacity exists in some fast regulation markets for BESS. For instance, 0.1 MW is the basic threshold for BESS to access the PJM market.

Here, we assume a BTM BESS will not influence the regulating price and all bidding capacities from the BESS are

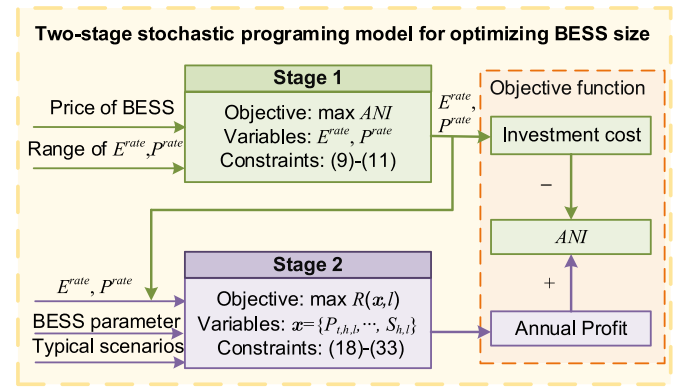


Fig. 1. Two-stage stochastic programming framework for optimizing BESS size.

successful. According to the PJM market rule, the regulation revenue  $R_h^{FR}$  in the  $h$  hour is given in (4). When the feasible capacity of BESS  $C_h^{bid}$  does not reach the lower threshold  $C_{h,lb}^{bid}$ , i.e., 0.1 MW, BESS will not perform the frequency regulation in the  $h^{th}$  hour.

$$R_h^{FR} = \begin{cases} 0 & 0 \leq C_h^{bid} < C_{h,lb}^{bid} \\ \sigma_h^{FR} C_h^{bid} \delta_h & C_{h,lb}^{bid} \leq C_h^{bid} \leq P_{rate} \end{cases} \quad (4)$$

The score  $\delta_h$  is an index to remark the comprehensive performance of BESS tracking the regulating signal in the  $h$  hour, which typically considers three performances: correlation, delay, and precision [31]. Here, we only focus on the precision score by neglecting other indexes as (5), because correlation and delay scores of BESS are usually close to 1 [11].

$$\delta_h = 1 - \frac{1}{T_1} \sum_{t_1=1}^{T_1} \left| \frac{P_{t_1,h} + C_h^{bid} f_{t_1,h}}{C_h^{bid} f_{t_1,h}} \right| \quad (5)$$

where,  $f$  represents the regulation signal that varies between  $[-1, 1]$ .

## III. PROBLEM FORMULATION

To make a robust and informed decision on BESS investment, a two-stage stochastic programming framework, which considers the uncertainty of operating scenarios, is proposed in this paper. Fig. 1 displays the overall framework of the proposed methodology. In Stage 1, the BESS size is optimized to maximize  $ANI$ , which is associated with both the investment cost and revenue. To achieve an accurate and reliable BESS size, the operating strategy is optimized to maximize the revenue in Stage 2, which takes the corresponding BESS size and typical operating scenarios as the inputs.

### A. Stage 1: Sizing Optimization

The carefully designed size easily brings back a high return rate for private investors and avoids unused capacity costs. Thus, in view of the affordability of customers and the profitability across a variety of sizes, Stage 1 targets optimizing a BESS size for maximizing  $ANI$ . The planning level

optimization model is described as follows:

$$\max ANI = E \left[ \sum_{m \in M} R_m(\mathbf{x}, l) \right] - C^{inv} \quad (6)$$

$$C^{inv} = \left( \sigma^E E^{rate} + \sigma^P P^{rate} \frac{r(1+r)^N}{(1+r)^N - 1} \right) \quad (7)$$

$$E \left[ \sum_{m \in M} R_m(\mathbf{x}, l_m) \right] = \sum_{m \in M} D_m \sum_{l_m \in L_m} p(l_m) R(\mathbf{x}, l_m) \quad (8)$$

$$\sigma^P P^{rate} + \sigma^E E^{rate} \leq C^{Bgt} \quad (9)$$

$$P^{lb} \leq P^{rate} \leq P^{ub} \quad (10)$$

$$E^{lb} \leq E^{rate} \leq E^{ub} \quad (11)$$

The objective function (6) aims to maximize the *ANI* of a BESS, which is achieved by minimizing the investment cost and maximizing the stackable revenue of the BESS over a year. The decision variables include the energy capacity  $E^{rate}$ , and power capacity  $P^{rate}$ . They are set as integer multiples of 10 kWh and 10 kW to realistically represent the BESS size and reduce the computing complexity. Equation (7) is the annual investment cost of BESS considering the annuity factor. In (8), the annual revenue based on typical operating scenarios is optimized in Stage 2. The investment budget is limited by (9). Equations (10) and (11) are constraints to prevent the searched energy and power capacity from violating the upper and lower limitations in the optimization process.

### B. Stage 2: BESS Operation Optimization

In this stage, the operating strategy of the BESS providing stackable services: energy arbitrage, peak shaving, and frequency regulation is designed to boost the economic revenue. The objective function of the established stochastic programming model is to maximize the monthly net revenue  $R_m$  over a year, which considers the BESS degradation cost and the uncertainty of operating scenarios, as shown in (12). To keep formulas concise, the subscript  $m$  is omitted. In the process, the BESS operator needs to determine and assign the time  $s_h$  and capacity  $P_{t,h}$  for different services as well as the peak shaving threshold  $P^{thr}$  for the month. The decision variables in the operating stage include  $\mathbf{x} = \{P_{t,h,l}, P_{t,h,l}^C, P_{t,h,l}^d, P^{thr}, P_{t,h,l}^{FR}, P_{t,h,l}^{EM}, C_{h,l}^{bid}, s_{h,l}\}$ .

$$\max R(\mathbf{x}, l) = \max \sum_{l \in L} p(l) \left\{ R^{EM}(\mathbf{x}, l) + R^{FR}(\mathbf{x}, l) - C^{O\&M}(\mathbf{x}, l) \right\} \quad (12)$$

$$\begin{aligned} \sum_{l \in L} p(l) R^{EM}(\mathbf{x}, l) &= \sigma^{PS} (P^{PD} - P^{PD,BE}) \\ &+ D_m \sum_{l \in L} \sum_{h \in H} \sum_{t \in T} p(l) \sigma_{t,h,l}^{EA} P_{t,h,l} \Delta t \end{aligned} \quad (12a)$$

Since the regulation service is not compatible with other services at the same hour, a binary variable  $s_h$  is introduced to assign the time providing the three services. The relationship

of BESS power and time assigned to the energy management service and the regulation service is as follows:

$$P_{t,h,l} = (1 - s_{h,l}) P_{t,h,l}^{FR} + s_{h,l} P_{t,h,l}^{EM} \quad (13)$$

When  $s_h$  equals 0, BESS will participate in the regulation market in the  $h^{th}$  hour with the bidding capacity  $C_{h,l}^{bid}$ , where

$$P_{t,h,l}^{FR} = P_{t,h,l}, \quad C^{bid,lb} \leq C_{h,l}^{bid} \leq P^{rate} \quad (14)$$

$$P_{t,h,l}^{EM} = 0 \quad (15)$$

Otherwise, BESS will be assigned to other services,

$$P_{t,h,l}^{FR} = 0, \quad C_{h,l}^{bid} = 0 \quad (16)$$

$$P_{t,h,l}^{EM} = P_{t,h,l} \quad (17)$$

To make the optimization problem solvable, the above nonlinear relationship - the product of binary variable  $s_h$  and a continuous variable  $P_{t,h,l}^{FR}$  or  $P_{t,h,l}^{EM}$  in (13) and segmentation functions from (14) to (17) are converted into the following linear constraints:

$$0 \leq C_{h,l}^{bid} \leq P^{rate} \quad (18)$$

$$(1 - s_{h,l}) C^{bid,lb} \leq C_{h,l}^{bid} \leq (1 - s_{h,l}) P^{rate} \quad (19)$$

$$P_{t,h,l} - s_{h,l} P^{rate} \leq P_{t,h,l}^{FR} \leq P_{t,h,l} + s_{h,l} P^{rate} \quad (20)$$

$$-P^{rate} (1 - s_{h,l}) \leq P_{t,h,l}^{FR} \leq P^{rate} (1 - s_{h,l}) \quad (21)$$

$$-P^{rate} \leq P_{t,h,l}^{FR} \leq P^{rate} \quad (22)$$

$$-P^{rate} s_{h,l} \leq P_{t,h,l}^{EM} \leq P^{rate} s_{h,l} \quad (23)$$

$$-P^{rate} \leq P_{t,h,l}^{EM} \leq P^{rate} \quad (24)$$

The constraint in (25) is defined to protect the user side's power from violating the monthly peak shaving threshold, where  $P^{thr} \in \mathbb{R}_+^1$ .

$$P_{t,h,l}^{load} + P_{t,h,l} \leq P^{thr} \quad (25)$$

As (12a) and (25) shows,  $P^{thr}$  has a significant impact on the revenue of each typical operating scenario. Thus, it should be calculated by optimizing all scenarios simultaneously.

The constraints (26)–(30) are added to ensure that the exchanged power of the BESS is underneath the rated power capacity limitation in the operation process.

$$P_{t,h,l} = P_{t,h,l}^c + P_{t,h,l}^d \quad (26)$$

$$-P^{rate} \leq P_{t,h,l} \leq P^{rate} \quad (27)$$

$$0 \leq P_{t,h,l}^d \leq P^{rate} \quad (28)$$

$$-P^{rate} \leq P_{t,h,l}^c \leq 0 \quad (29)$$

The *SoC* is a common index utilized to reflect a BESS operating state, which is the ratio of the current energy to its rated energy capacity. Generally, *SoC* will be limited in a range  $[SoC^{min}, SoC^{max}]$  to conserve the lifetime of a BESS.

$$SOC^{lb} \leq SOC^{ini} - \sum_{h=1}^H \sum_{t=1}^T \frac{\left[ P_{t,h,l}^c \eta^c + P_{t,h,l}^d / \eta_d \right] \Delta t}{E^{rate}} \leq SOC^{ub} \quad (30)$$

The constraint in (31) is applied to remain the BESS state at the same value at the initial and final moment of a day.

$$\sum_{h=1}^H \sum_{t=1}^T \left[ P_{t,h,l}^c \eta^c + P_{t,h,l}^d / \eta^d \right] \Delta t = 0 \quad (31)$$

### C. BESS Degradation Cost

The BESS operating cost is a crucial factor influencing the operating and planning results, which is mainly described as degradation cost subjected to BESS behaviors. Besides, the operation and planning of BESS are related to its degradation process as stated in [39] and [40], where the impact of the degraded capacity and the loss of efficiency are explored. It is worth mentioning that this research primarily focuses on developing a novel planning framework for stackable services. Only the degradation cost is considered in the model to simplify reflecting the influence of degradation on the operating and planning results.

This paper follows the linear degradation model presented in [7]. A brief introduction is given here. Given a certain *SoC* region  $[SoC^{\min}, SoC^{\max}]$  to limit the battery operation, the degradation cost  $C^{de}$  is regarded as a linear function of the battery charging/discharging power. The degradation cost of per-MWh  $\sigma^{de}$  is a marginal constant, which is related to the battery cell price and cycle numbers that the BESS can be operated within *SoC* limitation.

$$\sigma^{de} = \frac{\sigma^E}{2N_{cycle}(SoC^{\text{ub}} - SoC^{\text{lb}})} \quad (32)$$

$$C_h^{O\&M} = C_h^{de} = \sigma^{de} \sum_{t=1}^T \left( |P_t^c \eta^c| + |P_t^d / \eta^d| \right) \Delta t \quad (33)$$

It is worth mentioning that there is no extra binary variable for avoiding the BESS simultaneous charge and discharge in (26), which is attributed to the form of  $C_h^{O\&M}$  in (33). If it happens, the revenue remains the same but the  $C_h^{O\&M}$  will increase, which is not allowed by the objective function (12).

In summary, a MILP model is formulated in this stage for optimizing the BESS operating strategy. It consists of the objective function (12) and constraints (18) to (33). It is worth mentioning that this is a long-term investment problem, thus the operating strategy is not to serve real-time operation.

### D. Summary of the Two-Stage Stochastic Programming Model

The proposed two-stage stochastic programming model is a MINLP problem. The non-linear term existing in constraints (19)–(21) and (23) is the product of the discrete variable  $P^{rate}$  in Stage 1 and the binary variable  $s_{h,l}$  in Stage 2. Besides, the model in this research is a large-scale optimization problem. The objective function of Stage 2 – annual stackable revenue is the sum of 12-month revenue, which means 12 MILP problems need to be optimized for numerous candidate BESS sizes separately. And for achieving the best monthly threshold of peak shaving,  $L$  typical operating scenarios are required to be optimized simultaneously for each month. The above factors make the computational burden of solving the two-stage stochastic programming model significant.

---

### Algorithm 1 Generate Typical Operating Scenarios

---

**Input:** Historical load profile and regulation signal in a year

**Output:** Typical operating scenarios with the required resolution and their associated probability in month  $m$

for  $m=1:12$

1. Input monthly load profile  $P_m^{load}=\{P_{1,m}^{load}, P_{2,m}^{load}, \dots, P_{D_m,m}^{load}\}$  and monthly regulation signal  $f_m=\{f_{1,m}, f_{2,m}, \dots, f_{D_m,m}\}$ . Where the daily data  $P_{d,m}^{load}$  or  $f_{d,m}$  represents a scenario.
2. Set the number of clustered load scenarios and reduced regulation scenarios as  $I$  and  $J$ , separately
3. Cluster load scenarios based on the K-means clustering method
4. The clustered load scenarios  $l_{i,m}^{load}$  and its probability  $p_{i,m}^{load}$ , are employed for modeling the uncertainty of load
5. Reduce the regulation scenarios based on the FSR algorithm
6. The reduced regulation scenarios  $t_{j,m}^{fre}$  and its probability  $p_{j,m}^{fre}$  are employed for modeling the uncertainty of regulation signal
7. Convert the clustered load scenarios and reduced regulation scenarios into ones with the required resolution
8. Generate  $L$  typical operating scenarios and the joint probability  $p(l)$  by combining  $I$  clustered load scenarios and  $J$  reduced regulation scenarios, where  $L=I \cdot J$

end

---

## IV. GENERATE TYPICAL OPERATING SCENARIOS

To account for the uncertainty of the load profile and the regulation signal, a scenario-based method is employed in this research. The generated typical operating scenarios with associated probabilities will be adopted as the input of Stage 2, aiming for an accurate estimation of the revenue. Furthermore, typical operating scenarios with the required resolution should be generated to balance the computational burden and revenue accuracy in Stage 2. To this end, a novel equivalent model which can convert the second-level regulation signal to the minute-level one is proposed, which aims to reduce the computational burden while keeping the accuracy of the regulation revenue.

### A. Generate Typical Operating Scenarios

Algorithm 1 illustrates the generation of monthly typical operating scenarios with the required resolution and their probability. The load scenarios are classified utilizing the K-means clustering method, which is detailed in [10]. The regulation scenarios are reduced using the forward scenario reduction (FSR) algorithm, which is based on [7] and [29].

### B. Equivalent Model

A compromising and consistent time step is adopted in Stage 2, targeting to reduce the computational time caused by dense regulation signals and improve the revenue accuracy of peak shaving and energy arbitrage based on profiles with low resolution. To this end, the load and frequency regulation scenarios with the required resolution  $\Delta t$  are required to be generated.

To reduce the time resolution of regulation signals and retain the accuracy of regulation results, we propose a novel equivalent method to convert the second-level regulation signal into

a minute-level signal. It is achieved by analyzing the influence of the regulation signal on the BESS operation. During regulation hours, the main concerns are usually on the regulation profit and BESS behavior caused by the signal. The profit consists of direct revenue and the caused degradation cost. The BESS behavior can be reflected by the variation of  $SoC$ , which is also related to the degradation cost. Besides, the  $SoC$  at the end hour ( $SoC^{end}$ ) determines the available capacity in the next hour.

Thus, the regulation revenue  $R^{FR}$ , degradation cost  $C^{de}$  and  $\Delta SoC$  are selected as the observed objects to reflect the influence of different signals on operating results. To simplify the issue, the conducting process is based on the assumption that the BESS can completely follow the hourly signal at first. It means the performance score is equal to 1 in (5). Thus, the relationship between BESS power and signal can be represented as:

$$P_{t_1,h} + C_h^{bid} f_{t_1,h} = 0 \quad (34)$$

The  $\Delta SoC$  during a time interval  $\Delta t$  with sampling time  $\Delta t_1$  and  $\Delta t$  are shown in (35) and (36), separately.

$$\begin{aligned} \Delta SoC_{\Delta t_1, \Delta t} &= - \sum_{t_1 \in t} \left( P_{t_1,h}^c \eta^c + P_{t_1,h}^d / \eta_d \right) \Delta t_1 / E^{rate} \\ &= C_h^{bid} \sum_{t_1 \in t} \left( f_{t_1,h}^+ \eta^c + f_{t_1,h}^- / \eta_d \right) \Delta t_1 / E^{rate} \end{aligned} \quad (35)$$

$$\begin{aligned} \Delta SoC_{\Delta t, \Delta t} &= - \left( P_{t_1,h}^c \eta^c + P_{t_1,h}^d / \eta_d \right) \Delta t / E^{rate} \\ &= C_h^{bid} f_{t_1,h} \Delta t / E^{rate} \end{aligned} \quad (36)$$

To maintain the value of  $\Delta SoC_{\Delta t}$  constant, (35) should equal (36). Thus, the first signal feature is denoted as follows:

$$f_{t_1,h}^1 = f_{t_1,h} = \sum_{t_1 \in t} \left( f_{t_1,h}^+ \eta^c + f_{t_1,h}^- / \eta_d \right) \Delta t_1 / \Delta t \quad (\Delta t > \Delta t_1) \quad (37)$$

The  $\Delta SoC$  during  $\Delta t$  in the  $h^{th}$  hour based on the first signal feature can be represented as:

$$\Delta SoC_{\Delta t} = C_h^{bid} f_{t_1,h}^1 \Delta t / E^{rate} \quad (38)$$

As (4) presents, the regulation revenue is related to the performance score, since the bidding capacity and regulation price remain the same. In the condition that BESS can completely follow the regulation signal, it will achieve the same regulation revenue.

Similarly, by observing the degradation cost during  $\Delta t$  in the  $h^{th}$  hour, the following relationship is obtained.

$$\begin{aligned} C_{\Delta t_1, \Delta t}^{de} &= \sigma^{de} \sum_{t_1 \in t} |P_{t_1,h}^{FR}| \Delta t_1 \\ &= \sigma^{de} C_h^{bid} \sum_{t_1 \in t} \left( |f_{t_1,h}^+ \eta^c| + |f_{t_1,h}^- / \eta_d| \right) \end{aligned} \quad (39)$$

$$C_{\Delta t, \Delta t}^{de} = \sigma^{de} |P_{t_1,h}^{FR}| \Delta t = \sigma^{de} C_h^{bid} \left( |f_{t_1,h}^+ \eta^c| + |f_{t_1,h}^- / \eta_d| \right) \Delta t \quad (40)$$

The second signal feature is as follows, which can equivalently reflect the BESS hourly degradation cost.

$$f_{t_1,h}^2 = |f_{t_1,h}^+ \eta^c| + |f_{t_1,h}^- / \eta_d| = \sum_{t_1 \in t} \left( |f_{t_1,h}^+ \eta^c| + |f_{t_1,h}^- / \eta_d| \right) \Delta t_1 / \Delta t \quad (41)$$

Thus, when the BESS can completely follow the signal, the degradation cost during  $\Delta t$  is:

$$C_{\Delta t}^{de} = \sigma^{de} C_h^{bid} f_{t_1,h}^2 \Delta t \quad (42)$$

Considering the situation that BESS does not respond to the signal, the performance score is introduced to revise  $\Delta SoC$  and  $C^{de}$  during  $\Delta t$  as:

$$\begin{aligned} \Delta SoC_{\Delta t} &= C_h^{bid} f_{t_1,h}^1 \delta_{t_1,h} \Delta t / E^{rate} \\ &= \left( C_h^{bid} f_{t_1,h}^1 - |P_{t_1,h}^{FR} + C_h^{bid} f_{t_1,h}^1| \right) \Delta t / E^{rate} \end{aligned} \quad (43)$$

$$\begin{aligned} C_{\Delta t}^{de} &= \sigma^{de} C_h^{bid} f_{t_1,h}^2 \delta_{t_1,h} \Delta t / \Delta t \\ &= \sigma^{de} \left( C_h^{bid} f_{t_1,h}^2 - |P_{t_1,h}^{FR} - C_h^{bid} f_{t_1,h}^1 / f_{t_1,h}^1 f_{t_1,h}^2| \right) \Delta t_1 / \Delta t \end{aligned} \quad (44)$$

In summary, the two features  $f^1$  and  $f^2$  are introduced to replace the original signal, which can convert the second-level signal to any minute-level signal with approximate regulating results.

Take the month  $m$  as an example, the procedure of generating typical operating scenarios with the required resolution  $\Delta t$  is demonstrated in Fig. 2. The  $\Delta t$  is selected based on the duration period of the peak demand charge, which is usually 15 minutes. Since the time resolution of load profiles is usually an hour, linear interpolation is employed to generate ones with the resolution  $\Delta t$ . The proposed equivalent model is employed for generating equivalent regulation scenarios with the required resolution  $\Delta t$ . Finally,  $L$  typical operating scenarios with the required resolution are generated, which combine  $I$  load scenarios and  $J$  regulation scenarios.

## V. THE SOLUTION METHOD

As stated in Section II.D, the proposed two-stage stochastic programming model is a large-scale MINLP problem, which is hard to be solved directly by the classical optimization methods in an acceptable time. The hybrid algorithm combining the heuristic algorithm and the MILP has been demonstrated to be a viable approach for solving similar MINLP problems in BESS planning [16], [33], and [36]. Therefore, to alleviate the computational burden, this research employs a GA-MILP hybrid algorithm that splits the two-stage stochastic programming model into two parts for the solution. The BESS sizes searched by GA in Stage 1 are employed as the known constants in Stage 2. This approach obviates dealing with the non-linear term in constraints, thereby reducing the computational complexity. Furthermore, a strategy based on a filter and a recorder is proposed to be embedded into the hybrid algorithm to speed up the solution. The diagram of the hybrid algorithm is described in Fig. 3, where  $g$  denotes the times of GA running,  $k$  is the index of population generated by GA, and  $n$  is the index of chromosome in a population.

$$X = X^{\min} + Decimal(X_b) \frac{(X^{\max} - X^{\min})}{2N_b - 1} \quad (45)$$

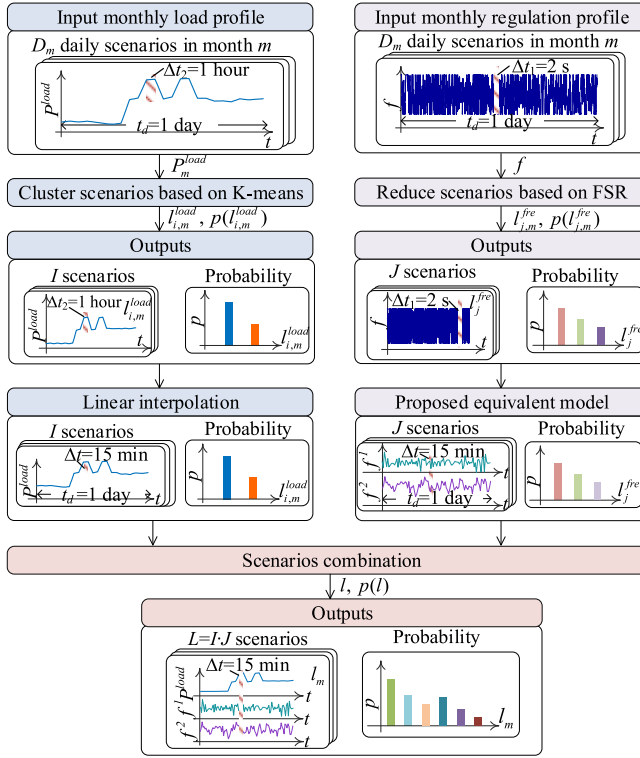


Fig. 2. Diagram of generating typical operating scenarios with the required time step.

In the first run of GA, an initial population is generated by GA at first. The binary encoding method is employed in this paper. The initial population includes  $N$  chromosomes  $C = \{C_1, C_2, \dots, C_N\}$  that is in binary format, representing a group of decimal candidate solutions  $S = \{S_1, S_2, \dots, S_N\}$ . Where  $S_n = \{E_n^{\text{rate}}, P_n^{\text{rate}}\}$  represents a type of BESS size. The conversion between the binary format  $X$  and the decimal format  $X_b$  of the decision variable is realized based on (45). Then, the BESS size  $S_n$ , which satisfies the constraints (9)–(11) in Stage 1, is sent to the next step for calculating the corresponding fitness function  $\text{ANI}(S_n)$ .  $\text{ANI}(S_n)$  is calculated based on (6). Among them, the capital investment cost  $C^{\text{inv}}(S_n)$  is calculated based on (7) in Stage 1 by taking  $S_n$  and BESS price as inputs. In Stage 2, the MILP model with the objective function (12) is optimized for solving the corresponding stackable revenues  $R(S_n)$ , which takes  $S_n$  and typical operating scenarios with associated probability as inputs. A commercial solver Gurobi is employed to solve the MILP model in Stage 2 to ensure the accuracy of the stackable revenue. Once the  $\text{ANI}$  calculation is completed for all chromosomes in a population, the stopping criterion is evaluated. If the criterion is not met, GA generates new offspring by executing the selection, crossover, and mutation on chromosomes in binary format. In order to minimize investment risks, GA will be executed multiple times to increase the probability of obtaining the global optimum.

In view of the characteristics of GA, fitter chromosomes have a higher chance of being selected as parents for reproduction, passing on their advantageous traits to the next generation. It leads to a large number of identical chromosomes in the single run of GA with the evolution of the

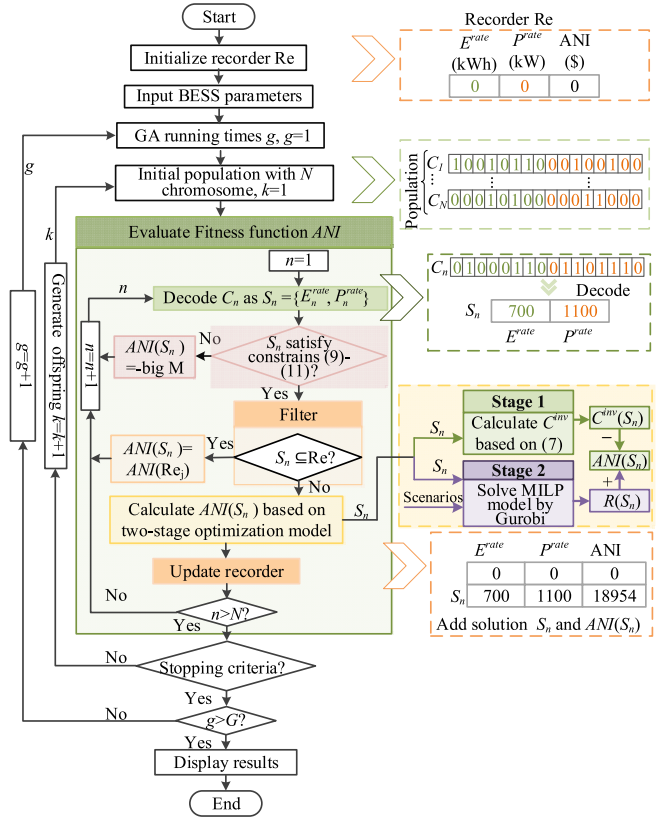


Fig. 3. A diagram illustrating a hybrid algorithm for solving the two-stage stochastic programming framework.

population. Besides, the solution of MILP is time-consuming. Solving recurring optimization problems can thus lead to significant computational overhead. As Fig. 3 shows, the strategy based on a recorder and a filter are incorporated in the GA-MILP hybrid algorithm, which eliminates the redundant computation of the fitness function for identical chromosomes in the single run and multiple runs of GA. The recorder keeps track of all generated BESS sizes and the corresponding optimized results. The filter will identify whether a size exists in the recorder. If yes, the corresponding fitness function value will be assigned to the size to avoid the redundant calculation. In addition, it brings extra advantages: a) the relationship between BESS size and  $\text{ANI}$  will be clearly observed by the recorder, which can be used for cost-economic analysis; b) it provides a clear view, which helps to narrow searched boundaries of BESS size, further fasten the optimal process and make the solution approach to be the global optimal one.

## VI. NUMERICAL ANALYSIS

In this section, the BESS sizing optimization is based on one-year industrial load profile and frequency regulation data from the PJM market. The performance of the proposed methods is analyzed and validated.

### A. Parameters Setup

The customer-side power consumption data is from a plastic manufacturing industry lasting for one year with a sampling time of 1 hour [41]. Fig. 4 shows the monthly load profile

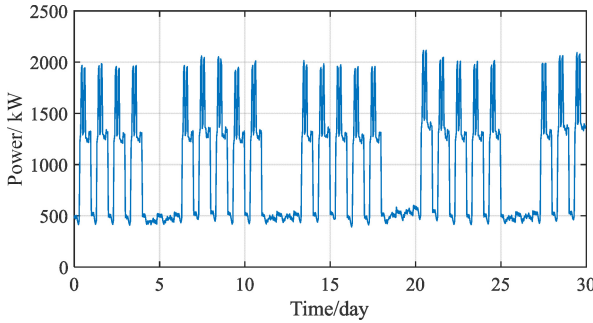


Fig. 4. Real industrial load profile of one month.

TABLE I  
ELECTRICITY PRICE FOR LARGE INDUSTRIAL CUSTOMERS

Energy charge (\$/kWh)	Demand charge (\$/kW)
On-Peak period (10:00-15:00) Off-Peak period (0:00-9:00) (16:00-23:00)	(500 kW < $P^{load}$ < 2999 kW)
0.0636	0.1044

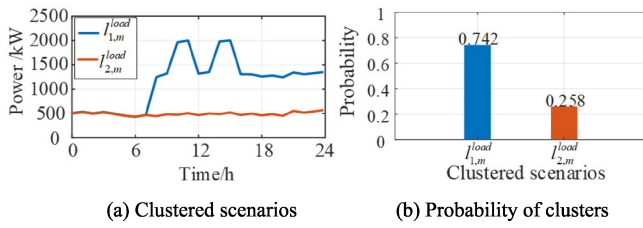


Fig. 5. Clustered load scenarios and probability in a month.

of the industry, where a bimodal trend appears on weekdays. The number of clustered load scenarios  $I$  is set as 2, since it exhibits distinct differences between weekdays and weekends and similar patterns on weekdays or weekends. The number of clustered load scenarios should be increased when different load profiles with more uncertainty are employed. The time-of-use energy price and demand charge price for industrial customers are listed in Table I [42]. The demand charge is calculated based on the load profile with the time step of 15 minutes, which is also the resolution of the stochastic programming model in Stage 2. Take the load profile in Fig. 4 as an example, its clustered load scenarios with associated probabilities are shown in Fig. 5.

The information related to frequency regulation is taken from the PJM market in 2020, including the regulation signal with a resolution of two seconds [43] and hourly regulation prices [44]. Here, the uncertainty of the daily price is neglected to simplify the planning problem, which is replaced by the average monthly regulation price for each hour. The number of reduced regulation scenarios  $J$  is set as 3 in the FSR algorithm for every month. For the example month, the equivalent regulation scenarios with the resolution of 15 minutes and their probabilities are shown in Fig. 6. Finally, there are 6 typical operating scenarios for a month, defined as a combination of 2 load scenarios and 3 regulation scenarios. The probability of typical operating scenarios in 12 months is listed in Table IV.

As a promising battery technology, the lithium ferro-phosphate (Li-LFP) battery, whose parameters are listed in Table II, is selected for providing stackable services in this

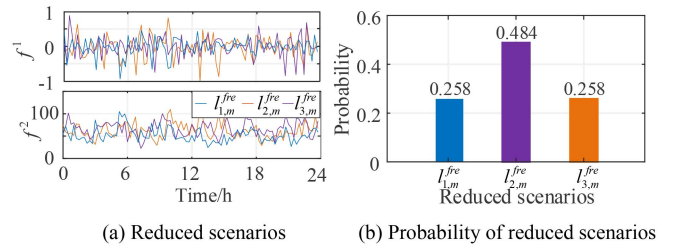


Fig. 6. Reduced regulation scenarios and probability in a month.

TABLE II  
PARAMETERS OF LITHIUM FERRO-PHOSPHATE (Li-LFP) BATTERY

Li-LFP Parameters	Values
Capital power cost (\$/kW)	800
Capital energy cost (\$/kWh)	300
Efficiency (%)	95
Range of SOC (%)	15-90
Lifetime (year)	10

TABLE III  
INITIAL PARAMETERS FOR REGULATION

BESS size	Regulation price	SoC limitation	$C^{bid}$
1 MW, 1 MWh	30 \$/MW	[15%, 90%]	1 MW

TABLE IV  
PROBABILITY OF TYPICAL OPERATING SCENARIOS

Probability	Typical operating scenarios						
	1	2	3	4	5	6	
Month	1	0.183	0.343	0.183	0.075	0.14	0.075
	2	0.079	0.128	0.079	0.197	0.32	0.197
	3	0.14	0.075	0.075	0.343	0.183	0.183
	4	0.196	0.342	0.196	0.071	0.124	0.071
	5	0.156	0.083	0.083	0.328	0.175	0.175
	6	0.342	0.196	0.196	0.124	0.071	0.071
	7	0.359	0.191	0.191	0.125	0.067	0.067
	8	0.328	0.175	0.175	0.156	0.083	0.083
	9	0.342	0.196	0.196	0.124	0.071	0.071
	10	0.183	0.343	0.183	0.075	0.14	0.075
	11	0.187	0.327	0.187	0.08	0.14	0.08
	12	0.359	0.191	0.191	0.125	0.067	0.067

paper. The predefined discretization scheme for the BESS size is based on the following parameters:  $E^{lb} = 100$  kWh,  $E^{ub} = 2500$  kWh,  $\Delta E = 10$  kWh,  $P^{lb} = 100$  kW,  $P^{ub} = 2500$  kW,  $\Delta P = 10$  kW.

### B. Performance of the Equivalent Model

In this section, an experiment is designed to illustrate the effectiveness of the proposed equivalent regulation signal model. It compares the regulation results of the real regulation signal with that of the proposed equivalent signal model, and the signal model utilized in [14] (take average signal every 15 minutes) and [24] (take a signal every 15 minutes).

To examine the difference between the three methods, 24 group samples from a daily typical regulation scenario are selected to compare the regulation results, where each hourly regulation signal is treated as a group of samples. Take the 1<sup>st</sup> group of signals as an instance, the real signal, the proposed equivalent signal, and the signal models

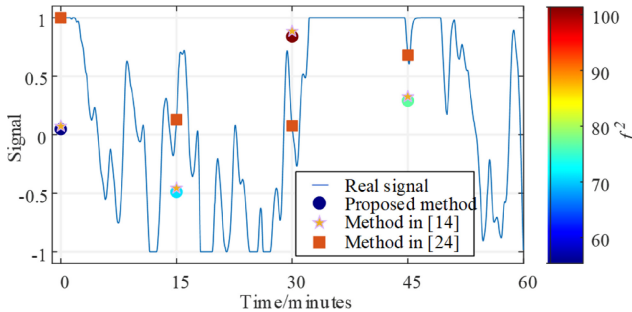


Fig. 7. 1<sup>st</sup> group of frequency regulation signals and three types of equivalent signals. The blue line is the real signal whose sampling time is 2 s. Generated signals with a resolution of 15 min based on the proposed method are solid circles with different colors. The value of ordinate denotes  $f^1$ , and its color means the value of  $f^2$ . Regulation signals generated based on [14] are denoted by the pentagons. The squares represent the generated signals based on [24].

TABLE V  
REGULATION RESULTS OF BESS BASED ON  
DIFFERENT EQUIVALENT SIGNALS

Initial SoC	MAPE	Proposed method	Method based on Ref. [14]	Method based on Ref. [24]
50%	R <sup>FR</sup> /%	<b>0.66</b>	36.69	12.57
	C <sup>de</sup> /%	<b>1.05</b>	61.36	20.62
	ΔSoC/%	<b>1.69</b>	2.46	44.28
80%	R <sup>FR</sup> /%	<b>3.34</b>	33.87	12.41
	C <sup>de</sup> /%	<b>1.79</b>	62.52	26.49
	ΔSoC/%	<b>1.21</b>	2.02	23.87

based on [14] and [24] are drawn in Fig. 7. In the compared experiments, the same initial conditions are adopted for all calculations as listed in Table III. The results in the two different conditions are observed, where in one condition we set the initial SoC as 50%, and in another condition, the initial SoC is set as 80%. Considering the varying scales of regulation results  $R^{FR}$ ,  $C^{de}$ , and  $ΔSoC$ , the mean absolute percentage error (MAPE), which provides a more intuitive vision compared with the root mean squared error or the mean absolute error, is selected for showing the performance of different models. The MAPE of 24 groups of regulation results is summarized in Table V.

In the first case, the initial SoC is assumed to be 50%, which allows the BESS to fully follow the regulation signal in most cases. As Fig. 8 (a) shows, the performance score calculated based on (5) is near to 100 based on all real signals, which is consistent with the hypothetical situation. It is worth mentioning that  $f^1$  generated by the proposed equivalent model is adopted as  $f$  in (5) for the performance score calculation, as shown in (43). In terms of the BESS behavior, as shown in Fig. 5 (b), we can find that the SoC based on the proposed method is basic match with the real SoC. The method in [14] achieved similar results, while there are large errors when the method presented in [24] is applied. It proves the effectiveness of the first signal feature. As for the revenue and degradation cost, the approachable results are also realized based on the proposed model as Fig. 8 (c) and (d) demonstrate. Meanwhile, one can observe the degradation costs are always

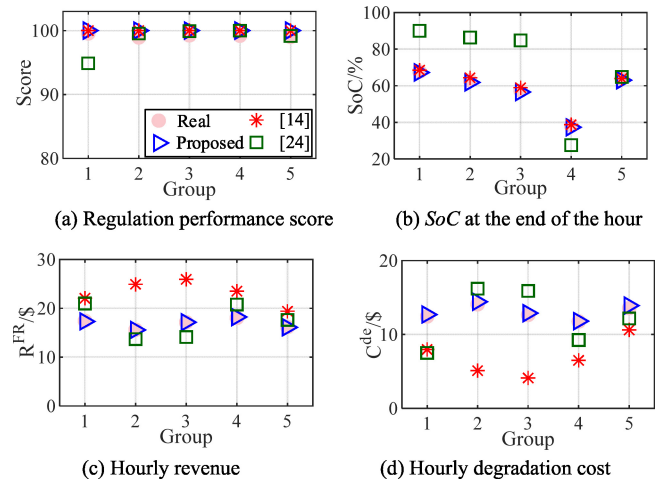


Fig. 8. Regulation results of four types of signals when  $SoC^{ini}$  is 50%.

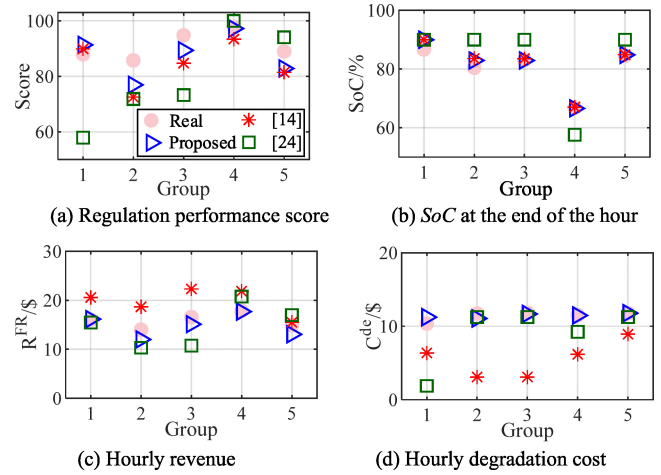


Fig. 9. Regulation results of four types of signals when  $SoC^{ini}$  is 80%.

underestimated based on [14], which is due to the fact that the fluctuations of the signal between  $[-1,1]$  are decreased when the average signal is adopted. It leads to an overestimation of the regulation revenue, which will further result in a higher power-to-energy ratio in the size of the BESS. As Table V shows, the results based on [24] also exist large errors.

It is possible that the BESS cannot completely follow the real regulation signal. To simulate this situation, the initial SoC is set as an extreme condition of 80%, and assume the BESS still participates in the regulation market as 1 MW. Fig. 9 shows the regulation results of five groups of these signals, which performance scores of the five groups' signals are different and lower than 100, as shown in Fig. 9 (a). Even in this condition, the approachable regulation results are still achieved based on the proposed method, as presented in Fig. 9 (b)-(d) and Table V. It shows better performance compared to the two other methods.

The superiority of the proposed equivalent model is that it can convert the second-level signal into the minute-level without largely scarify the accuracy of the regulation results whatever the BESS can completely follow or not the regulation signal.

TABLE VI  
GA PARAMETERS AND STOPPING CRITERIA

GA Parameters	Values
Number of decision variables	2
$N_b$ for $E^{rate}$ and $P^{rate}$ in 1 <sup>st</sup> searching horizon	8, 8
$X^{\min}, X^{\max}$ for $E^{rate}$ in 1 <sup>st</sup> searching horizon	0 kWh, 2550 kWh
$X^{\min}, X^{\max}$ for $P^{rate}$ in 1 <sup>st</sup> searching horizon	0 kW, 2550 kW
$N_b$ for $E^{rate}$ and $P^{rate}$ in 2 <sup>nd</sup> searching horizon	6, 7
$X^{\min}, X^{\max}$ for $E^{rate}$ in 2 <sup>nd</sup> searching horizon	300 kWh, 930 kWh
$X^{\min}, X^{\max}$ for $P^{rate}$ in 2 <sup>nd</sup> searching horizon	500 kW, 1770 kW
Generation gap	0.9
Mutation rate	0.01
Crossover rate	0.7
Population size	20
Termination criteria and value	Stall generation-30

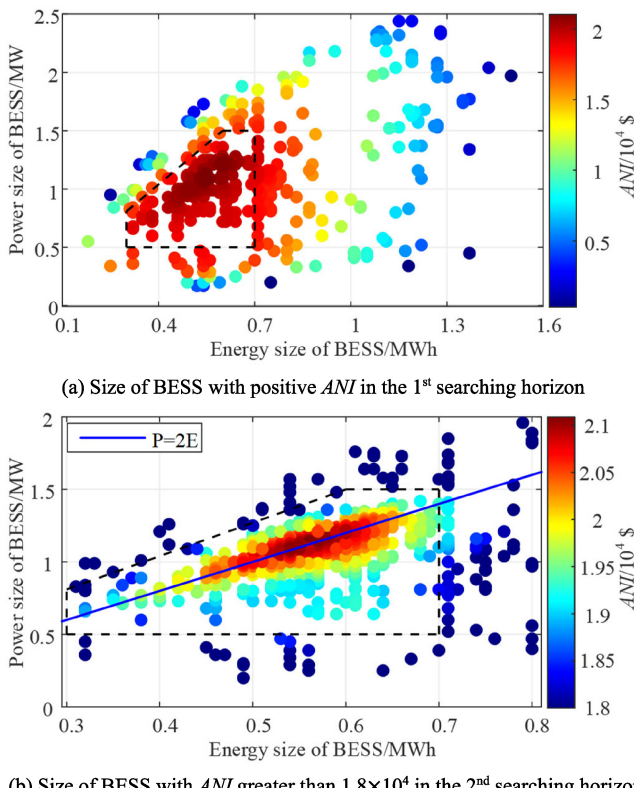


Fig. 10. BESS size and corresponding ANI searched by the hybrid algorithm.

### C. Optimization of BESS Size

GA runs firstly five times within the predefined sizing horizon to solve the two-stage stochastic programming framework. The concrete parameters of GA are listed in Table VI. By utilizing the encoding parameters in Table VI, each chromosome can accurately represent a type of BESS size in the predefined discretization scheme, thereby ensuring a precise and efficient search towards the optimal solution. All searched sizes and the corresponding ANI are stored in the recorder, where BESS sizes with positive ANI are shown in Fig. 10 (a). It can be found that an obvious distribution pattern exists in sizes and ANI. On this basis, the searched limitation of BESS size can further be narrowed. Take ANI greater than  $1.8 \times 10^4$  \$ as a dividing line, the new boundaries

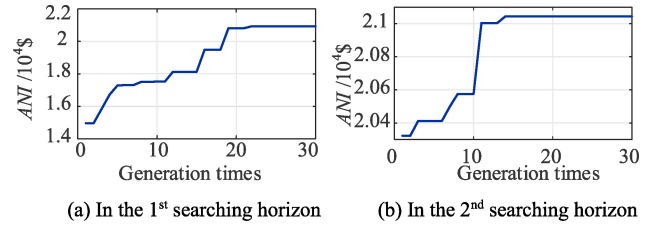


Fig. 11. Examples of GA convergence process in the two searching horizons.

TABLE VII  
RESULTS OF OPTIMAL SIZE AND STACKED REVENUE

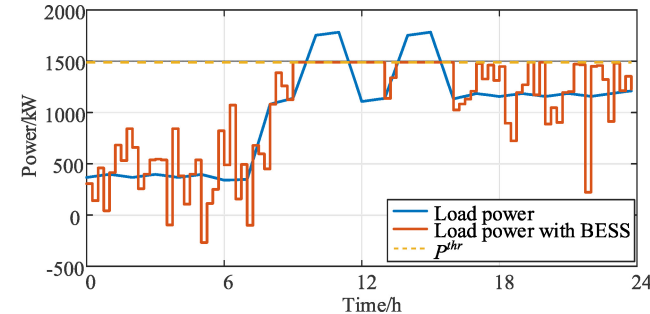
	Values	Values
ANI (\$)	21,030	Optimal size MWh, 0.54
Annual cost (\$)	210,991	Investment cost (\$) 140,487
		Operation cost (\$) 70,504
Annual revenue (\$)	232,021	Energy Arbitrage (\$) -2,265
		Peak shaving revenue (\$) 29,622
		Regulation revenue (\$) 204,664

include  $E^{lb} = 300$  kWh,  $E^{ub} = 700$  kWh,  $P^{lb} = 500$  kW,  $P^{ub} = 1500$  kW, and  $P = 2.3E + 0.12\text{MW}$ , which form a pentagon in Fig. 10. Then the GA runs three times in the new sizing horizon for searching the global optimal solution, as shown in Fig. 10 (b). As an example, GA convergence process in the predefined sizing horizon and narrowed horizon are presented in Fig. 11.

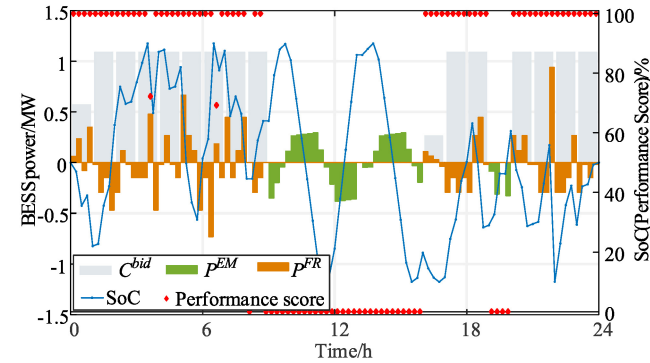
*Economic analysis:* Fig. 10 (a) demonstrates those BESS sizes with positive ANI, which reflects the economic feasibility of varied sizes of BESS and the trend of ANI with BESS size. Obviously, with the increase in size, the ANI will firstly rise and then decrease, since the revenue created by the increased size cannot cover its investment cost. It proves the optimal BESS size is a compromise between profit and investment cost. Notable, when the energy sizes are larger than 1.5 MWh, BESS cannot achieve positive ANI anymore. It shows the importance of reasonable planning and incorporating the investment cost and operational cost into the economic analysis.

*Optimal results and stacked revenue:* When the initial budget limitation is larger than 1 M\$, the optimal size of BESS appears in the solution with an energy capacity of 0.54 MWh and power capacity of 1.09 MW, where the initial investment cost is 1.4 M\$ and ANI is 21,030 \$. According to Fig. 10 (b), we can deduce that the solved BESS size is the global optimum based on the intensive search. When the investment budget is lower than 1 M\$, the optimal size is 0.38 MWh and 0.77 MW with the investment cost 0.99 M\$ and ANI 19,648 \$.

Take the BESS size with the highest ANI as an example for analysis, the investment cost and the bringing revenues are recorded in Table VII. One can observe the highest revenue is from the regulation service, which brings revenue accounting for 88%. It leads to that the BESS with high power size usually shows better economic performance than that with high energy. In addition, a straight line is obtained by fitting solutions with superior economic performance as shown in Fig. 10 (b), where the power size is around 2 times of the energy size.



(a) Load power demand with and without BESS.



(b) BESS power assigned to three services, SoC variation and regulation score.

Fig. 12. BESS performs stackable services in a typical operating scenario.

The high degradation cost is presented in Table VII since the BESS continuously follows the regulation signal leading to frequent operation behavior. While the second highest benefits are obtained through peak shaving. Under the given electricity price in Table I, energy arbitrage cannot bring back the profit if the subsidy of BESS is not considered. Based on the optimized size, neither the benefits of regulation nor the benefits of energy management fully repay the total costs. However, the total revenue from the stackable services is 1.1 times of the total costs.

Based on the optimized BESS size of 0.54 MWh/ 1.09 MW, the operating strategy of a typical day in January is demonstrated in Fig. 12. As Fig. 12 (a) shows, the original peak load is up to 1783 kW with demand charge of 21,182 \$. When the BESS is installed, the load in peak periods is shaved to the threshold, which is optimized as 1488 kW with a demand charge of 17,677 \$. Also, the load power plus the BESS power in other periods cannot surpass the set threshold. Through the SoC curve in Fig. 12 (b), one can obviously observe that the BESS is charged in advance to ensure that the BESS has sufficient capacity for performing peak shaving during peak periods. In other periods, BESS prefers to participate in the regulation market due to its higher revenue. It can be observed that BESS usually employs its rated power capacity when participating in the regulation service. However, during specific hours, it operates at a partial capacity in the regulation service, which is limited by the operating constraints and for achieving the maximum stackable revenue. It has been noted that the performance score of BESS occasionally falls below 100%, which is attributed to the SoC limitation of BESS.

TABLE VIII  
NUMBER OF SIZES WHOSE ANI NEEDS TO BE CALCULATED

Number of BESS sizes	GA-MILP hybrid algorithm		Saved time
	With strategy	Without strategy [28], [36]	
Run GA 1 <sup>st</sup> time	179	600	70.2%
Run GA total 5 times	531	3000	82.3%

#### D. Computational Time Analysis

In this paper, the BESS planning is executed using MATLAB R2021a on the personal laptop with an Intel Core i5-10210U CPU and 16GB RAM. The MILP model is solved by commercial solver YALMIP and GUROBI 9.0.0 package.

Thanks to the regulation signal equivalent model, the granularity during a day is reduced to 96. On this basis, it spends around 4.5 hours to calculate the ANI for 20 types of BESS sizes, which are in the initial population of GA. Table VIII lists the number of BESS sizes whose fitness function ANI needs to be calculated in the predefined searching horizon. Thanks to the proposed strategy based on a filter and a recorder, the ANI of only 179 non-redundant sizes is required to be calculated when GA runs the first time, while the GA-MILP hybrid algorithm without this strategy [28], [36] needs to calculate ANI of 600 types of BESS sizes. We can infer that the proposed strategy can save around 70.2% calculating time in GA run single time rather than the algorithm in [28] and [36]. Similarly, when GA is run a total of five times, it allows a time saving of up to 82.3% by only calculating ANI of 531 types of BESS sizes. Obviously, it can speed up the solution in both single and multiple runs of GA.

## VII. CONCLUSION

In this paper, a profit-oriented sizing optimization method of BTM BESS has been proposed, where stackable services consisting of customer-side services, i.e., energy arbitrage, peak shaving, and a grid frequency regulation service are provided. The problem was formulated as a two-stage stochastic programming model to co-optimize the size and the operational strategy. A numerical analysis based on a real historical industrial load and regulation information was performed, which illustrated the following outcomes:

- Under the given electricity market rules, the revenue from regulation market was larger than that from other services, which led to the optimal power size of the BESS to be around 2 times of energy size.
- The proposed strategy based on a filter and a recorder was validated to enhance the efficiency of the GA-MILP hybrid algorithm for solving the MINLP model, saving up to 70.2% time compared to the case without the filter and recorder.
- The proposed two features of regulation signal with minute-level could effectively represent the original second-level signal with the MAPE of regulation revenue less than 3.34%. It maintained the accuracy of regulating scenarios and further preserved the effectiveness of planning. The method is easily applicable to other degradation models by replacing the second feature.

The proposed planning method is easily expandable to other similar planning work. The detailed BESS degradation model will be incorporated into future work to provide a more reliable planning result. Additionally, although this paper only considers the energy management services on the customer side, BESS can also coordinate with renewable generations to improve self-consumption or power supply reliability, which will be explored in future works.

### ACKNOWLEDGMENT

The authors gratefully acknowledge the contributions of Dr. Menglin Zhang at School of Automation, China University of Geosciences for her valuable and constructive comments for this document.

### REFERENCES

- [1] *Innovation Landscape Brief: Behind-the-Meter Batteries*, IRENA, Abu Dhabi, UAE, 2019, pp. 5–6.
- [2] T. Bowen and C. Gokhale-Welch, *Behind-the-Meter Battery Energy Storage: Frequently Asked Questions*, NREL, Golden, CO, USA, 2021.
- [3] A. Dougherty, B. Billings, N. Camacho, and K. Powell, “Improving the economics of battery storage for industrial customers: Are incentives enough to increase adoption?” *Electr. J.*, vol. 34, no. 9, Nov. 2021, Art. no. 107027.
- [4] L. Mauler, F. Duffner, W. G. Zeier, and J. Leker, “Battery cost forecasting: A review of methods and results with an outlook to 2050,” *Energy Environ. Sci.*, vol. 14, no. 9, pp. 4712–4739, Aug. 2021.
- [5] S. Englberger, A. Jossen, and H. Hesse, “Unlocking the potential of battery storage with the dynamic stacking of multiple applications,” *Cell Rep. Phys. Sci.*, vol. 1, no. 11, Nov. 2020, Art. no. 100238.
- [6] G. Fong, R. Moreira, and G. Strbac, “Economic analysis of energy storage business models,” in *Proc. IEEE Manchester PowerTech*, 2017, pp. 1–6.
- [7] Y. Shi, B. Xu, D. Wang, and B. Zhang, “Using battery storage for peak shaving and frequency regulation: Joint optimization for super-linear gains,” *IEEE Trans. Power Syst.*, vol. 33, no. 3, pp. 2882–2894, May 2018.
- [8] Y. Tian, A. Bera, M. Benidris, and J. Mitra, “Stacked revenue and technical benefits of a grid-connected energy storage system,” *IEEE Trans. Ind. Appl.*, vol. 54, no. 4, pp. 3034–3043, Jul./Aug. 2018.
- [9] M. B. Mustafa, P. Keatley, Y. Huang, O. Agbonaye, O. O. Ademulegun, and N. Hewitt, “Evaluation of a battery energy storage system in hospitals for arbitrage and ancillary services,” *J. Energy Storage*, vol. 43, Nov. 2021, Art. no. 103183.
- [10] X. Wang, F. Li, Q. Zhang, Q. Shi, and J. Wang, “Profit-oriented BESS siting and sizing in deregulated distribution systems,” *IEEE Trans. Smart Grid*, vol. 14, no. 2, pp. 1528–1540, Mar. 2023.
- [11] A. Awad, T. H. M. El-Fouly, and M. M. A. Salama, “Optimal ESS allocation for benefit maximization in distribution networks,” *IEEE Trans. Smart Grid*, vol. 8, no. 4, pp. 1668–1678, Jul. 2017.
- [12] Y. J. A. Zhang, C. Zhao, W. Tang, and S. H. Low, “Profit-maximizing planning and control of battery energy storage systems for primary frequency control,” *IEEE Trans. Smart Grid*, vol. 9, no. 2, pp. 712–723, Mar. 2018.
- [13] A. Alamri, M. Alowaifeer, and A. P. S. Meliopoulos, “Energy storage sizing and probabilistic reliability assessment for power systems based on composite demand,” *IEEE Trans. Power Syst.*, vol. 37, no. 1, pp. 106–117, Jan. 2022.
- [14] N. B. Arias et al., “Multi-objective sizing of battery energy storage systems for stackable grid applications,” *IEEE Trans. Smart Grid*, vol. 12, no. 3, pp. 2708–2721, May 2021.
- [15] C. Gu, J. Wang, Y. Zhang, Q. Li, and Y. Chen, “Optimal energy storage planning for stacked benefits in power distribution network,” *Renew. Energ.*, vol. 195, pp. 366–380, Aug. 2022.
- [16] M. Ma, H. Huang, X. Song, F. Peña-Mora, Z. Zhang, and J. Chen, “Optimal sizing and operations of shared energy storage systems in distribution networks: A bi-level programming approach,” *Appl. Energy*, vol. 307, Feb. 2022, Art. no. 118170.
- [17] M. Jaszcuzur, Q. Hassan, A. M. Abdulateef, and J. Abdulateef, “Assessing the temporal load resolution effect on the photovoltaic energy flows and self-consumption,” *Renew. Energ.*, vol. 169, pp. 1077–1090, May 2021.
- [18] U. G. K. Mulleriyawage and W. X. Shen, “Impact of demand side management on optimal sizing of residential battery energy storage system,” *Renew. Energ.*, vol. 172, pp. 1250–1266, Jul. 2021.
- [19] H. Zhao et al., “Resilience assessment of hydrogen-integrated energy system for airport electrification,” *IEEE Trans. Ind. Appl.*, vol. 58, no. 2, pp. 2812–2824, Mar./Apr. 2022.
- [20] Y. Zhang, T. Ma, P. E. Campana, Y. Yamaguchi, and Y. Dai, “A techno-economic sizing method for grid-connected household photovoltaic battery systems,” *Appl. Energy*, vol. 268, Jul. 2020, Art. no. 115106.
- [21] H. Masrur, A. Sharifi, M. R. Islam, M. A. Hossain, and T. Senju, “Optimal and economic operation of microgrids to leverage resilience benefits during grid outages,” *Int. J. Electr. Power Energy Syst.*, vol. 132, Nov. 2021, Art. no. 107137.
- [22] Y. Ding, Q. Xu, and Y. Huang, “Optimal sizing of user-side energy storage considering demand management and scheduling cycle,” *Electr. Power Syst. Res.*, vol. 184, Jul. 2020, Art. no. 106284.
- [23] S. Arabi-Nowdeh et al., “Multi-criteria optimal design of hybrid clean energy system with battery storage considering off- and on-grid application,” *J. Clean. Prod.*, vol. 290, Mar. 2021, Art. no. 125808.
- [24] J. Engels, J. Engels, B. Claessens, and G. Deconinck, “Optimal combination of frequency control and peak shaving with battery storage systems,” *IEEE Trans. Smart Grid*, vol. 11, no. 4, pp. 3270–3279, Jul. 2020.
- [25] Z. Wang and D. S. Kirschen, “Two-stage optimal scheduling for aggregators of batteries owned by commercial consumers,” *IET Gener. Transmiss. Distrib.*, vol. 13, no. 21, pp. 4880–4887, Nov. 2019.
- [26] Z. Wang, A. Negash, and D. S. Kirschen, “Optimal scheduling of energy storage under forecast uncertainties,” *IET Gener. Transmiss. Distrib.*, vol. 11, no. 17, pp. 4220–4226, Nov. 2017.
- [27] B. Cheng and W. B. Powell, “Co-optimizing battery storage for the frequency regulation and energy arbitrage using multi-scale dynamic programming,” *IEEE Trans. Smart Grid*, vol. 9, no. 3, pp. 1997–2005, May 2018.
- [28] Y. Zhang, A. Anvari-Moghadam, S. Peyghami, T. Dragicevic, Y. Li, and F. Blaabjerg, “Optimal sizing of behind-the-meter BESS for providing stackable services,” in *Proc. IEEE 13th Int. Symp. Power Electron. Distrib. Gener. Syst. (PEDG)*, 2022, pp. 1–6.
- [29] H. Su et al., “Optimization of customer-side battery storage for multiple service provision: Arbitrage, peak shaving, and regulation,” *IEEE Trans. Ind. Appl.*, vol. 58, no. 2, pp. 2559–2573, Mar./Apr. 2022.
- [30] B. Zhao, J. Ren, J. Chen, D. Lin, and R. Qin, “Tri-level robust planning-operation co-optimization of distributed energy storage in distribution networks with high PV penetration,” *Appl. Energy*, vol. 279, Dec. 2020, Art. no. 115768.
- [31] M. S. Javadi et al., “A two-stage joint operation and planning model for sizing and siting of electrical energy storage devices considering demand response programs,” *Int. J. Electr. Power Energy Syst.*, vol. 138, Jun. 2022, Art. no. 107912.
- [32] B. Zhang, P. Dehghanian, and M. Kezunovic, “Optimal allocation of PV generation and battery storage for enhanced resilience,” *IEEE Trans. Smart Grid*, vol. 10, no. 1, pp. 535–545, Jan. 2019.
- [33] A. S. A. Awad, T. H. M. El-Fouly, and M. M. A. Salama, “Optimal ESS allocation for load management application,” *IEEE Trans. Power Syst.*, vol. 30, no. 1, pp. 327–336, Jan. 2015.
- [34] A. Rathore and N. P. Patidar, “Optimal sizing and allocation of renewable based distribution generation with gravity energy storage considering stochastic nature using particle swarm optimization in radial distribution network,” *J. Energy Storage*, vol. 35, Mar. 2021, Art. no. 102282.
- [35] R. Li, W. Wang, Z. Chen, and X. Wu, “Optimal planning of energy storage system in active distribution system based on fuzzy multi-objective bi-level optimization,” *J. Modern Power Syst. Clean Energy*, vol. 6, no. 2, pp. 342–355, Mar. 2018.
- [36] D. Wu, Q. Gui, W. Zhao, J. Wang, S. Shi, and Y. Zhou, “Battery energy storage system (BESS) sizing analysis of bess-assisted fast-charge station based on double-layer optimization method,” in *Proc. IEEE 3rd Student Conf. Electr. Mach. Syst.*, 2020, pp. 658–662.
- [37] D. Wu, X. Ma, P. Baldacci, and D. Bhatnagar, “An economic assessment of behind-the-meter photovoltaics paired with batteries on the Hawaiian Islands,” *Appl. Energy*, vol. 286, Mar. 2021, Art. no. 116550.
- [38] X. Wang, F. Li, L. Bai, and X. Fang, “DLMP of competitive markets in active distribution networks: Models, solutions, applications, and visions,” *Proc. IEEE*, vol. 111, no. 7, pp. 725–743, Jul. 2023.

- [39] R. Nebuloni et al., "A hierarchical two-level MILP optimization model for the management of grid-connected BESS considering accurate physical model," *Appl. Energy*, vol. 334, Mar. 2023, Art. no. 120697.
- [40] M. Petrelli, D. Fioriti, A. Berizzi, and D. Poli, "Multi-year planning of a rural microgrid considering storage degradation," *IEEE Trans. Power Syst.*, vol. 36, no. 2, pp. 1459–1469, Mar. 2021.
- [41] F. Angizeh, A. Ghofrani, and M. Jafari, "Dataset on hourly load profiles for a set of 24 facilities from industrial, commercial, and residential end-use sectors," 2020. [Online]. Available: [https://dataminer2.pjm.com/feed/reg\\_market\\_results/definition](https://dataminer2.pjm.com/feed/reg_market_results/definition)
- [42] "View the (HT) large industrial—Demand 500-2,999 kw rate details," Turlock Irrigation District. 2022. [Online]. Available: <https://www.tid.org/customer-service/rates-rules/power-rates-rules/>
- [43] "PJM historical regulation market data," PJM. 2020. [Online]. Available: [https://dataminer2.pjm.com/feed/reg\\_market\\_results/definition](https://dataminer2.pjm.com/feed/reg_market_results/definition)
- [44] "RTO regulation signal data," PJM. 2020. [Online]. Available: <https://www.pjm.com/markets-and-operations/ancillary-services>



**Yichao Zhang** (Graduate Student Member, IEEE) received the B.Sc. and M.Sc. degrees in electrical engineering from Southwest Jiaotong University, Chengdu, China, in 2017 and 2020, respectively. She is currently pursuing the Ph.D. degree with AAU Energy, Aalborg University, Aalborg, Denmark.

Her research interests include energy storage system plan and control, uncertainty modeling, and frequency stability analysis.



**Amjad Anvari-Moghaddam** (Senior Member, IEEE) is currently an Associate Professor and a Leader of Intelligent Energy Systems and Flexible Markets Research Group with the Department of Energy, Aalborg University, Aalborg, Denmark, where he is also acting as the Vice-Leader of Power Electronic Control, Reliability and System Optimization and the Coordinator of Integrated Energy Systems Laboratory. He has (co)authored more than 280 technical articles, seven books, and 17 book chapters in the field. His research interests

include planning, control and operation management of microgrids, renewable/hybrid power systems, and integrated energy systems with appropriate market mechanisms.

Dr. Anvari-Moghaddam was the recipient of the 2020 DUO-India Fellowship Award, the DANIDA Research Fellowship Grant from the Ministry of Foreign Affairs of Denmark in 2018 and 2021, the IEEE-CS Outstanding Leadership Award 2018 (Halifax, NS, Canada), and the 2017 IEEE-CS Outstanding Service Award (Exeter, U.K.). He is an Associate Editor for several leading journals, such as the IEEE TRANSACTIONS ON POWER SYSTEMS, IEEE SYSTEMS JOURNAL, IEEE OPEN ACCESS JOURNAL OF POWER AND ENERGY, and IEEE POWER ENGINEERING LETTERS. He is the Vice-Chair of IEEE Denmark and IEEE-PES Danish Chapter and a Technical Committee Member of several IEEE PES/IES/PELS and CIGRE Working Groups.



**Saeed Peyghami** (Senior Member, IEEE) received the B.Sc., M.Sc., and Ph.D. degrees in electrical engineering from the Electrical Engineering Department, Sharif University of Technology, Tehran, Iran, in 2010, 2012, and 2017, respectively.

From 2015 to 2016, he was a Visiting Ph.D. Scholar with the Department of Energy, Aalborg University, Aalborg, Denmark. From 2017 to 2021, he was a Postdoctoral Research Fellow with Aalborg University. In 2019, he was a Visiting Researcher with Intelligent Electric Power Grids, Technology, Delft, The Netherlands. He is currently an Assistant Professor in electrical power engineering with Aalborg University. His research interests include reliability, control, and stability of power electronic-based power systems, and renewable energies.



**Yuan Li** (Graduate Student Member, IEEE) received the B.Sc. and M.Sc. degrees in electrical engineering from Southwest Jiaotong University, Chengdu, China, in 2017 and 2020, respectively. She is currently pursuing the Ph.D. degree with AAU Energy, Aalborg University, Aalborg, Denmark.

Her research interests include modeling of power converters, stability analysis of dc microgrid, and model predictive control for power converters.



**Tomislav Dragičević** (Senior Member, IEEE) received the M.Sc. and Industrial Ph.D. degrees in electrical engineering from the Faculty of Electrical Engineering, University of Zagreb, Zagreb, Croatia, in 2009 and 2013, respectively.

From 2013 to 2016, he was a Postdoctoral Researcher with Aalborg University, Aalborg, Denmark. From 2016 to 2020, he was an Associate Professor with Aalborg University. He was a Guest Professor with Nottingham University, Nottingham, U.K., during Spring/Summer of 2018. From 2020, he is a Professor with the Technical University of Denmark, Kongens Lyngby, Denmark. He has authored and coauthored more than 230 technical publications (more than 100 of them are published in international journals, mostly in IEEE), eight book chapters, and a book in the field. His research interests include application of advanced control, optimization and artificial intelligence-inspired techniques to provide innovative and effective solutions to emerging challenges in design, control, and cyber-security of power-electronics intensive electrical distributions systems and microgrids.

Dr. Dragičević is a recipient of the Koncar Prize for the Best Industrial Ph.D. Thesis in Croatia, a Robert Mayer Energy Conservation Award, and is the winner of an Alexander Von Humboldt Fellowship for experienced researchers. He serves as an Associate Editor for the IEEE TRANSACTIONS ON INDUSTRIAL ELECTRONICS, IEEE TRANSACTIONS ON POWER ELECTRONICS, IEEE EMERGING AND SELECTED TOPICS IN POWER ELECTRONICS, and the IEEE Industrial Electronics Magazine.



**Frede Blaabjerg** (Fellow, IEEE) received the Ph.D. degree in electrical engineering from Aalborg University, Aalborg, Denmark, in 1995.

He was with ABB-Scandia, Randers, Denmark, from 1987 to 1988. He became an Assistant Professor in 1992, an Associate Professor in 1996, and a Full Professor of Power Electronics and Drives in 1998. Since 2017, he has been a Villum Investigator. He is honoris causa with University Politehnica Timisoara, Romania, and Tallinn Technical University, Estonia. He has published more than 600 journal papers in the fields of power electronics and its applications. He is the coauthor of four monographs and editor of ten books in power electronics and its applications. His current research interests include power electronics and its applications, such as in wind turbines, PV systems, reliability, harmonics, and adjustable speed drives.

Dr. Blaabjerg received 32 IEEE Prize Paper Awards, the IEEE PELS Distinguished Service Award in 2009, the EPE-PEMC Council Award in 2010, the IEEE William E. Newell Power Electronics Award 2014, the Villum Kann Rasmussen Research Award 2014, the Global Energy Prize in 2019, and the 2020 IEEE Edison Medal. He was the Editor-in-Chief of the IEEE TRANSACTIONS ON POWER ELECTRONICS from 2006 to 2012. He has been a Distinguished Lecturer for the IEEE Power Electronics Society from 2005 to 2007 and the IEEE Industry Applications Society from 2010 to 2011 as well as 2017 to 2018. From 2019 to 2020, he served as President for IEEE Power Electronics Society. He is the Vice-President of the Danish Academy of Technical Sciences too. He is nominated in 2014–2019 by Thomson Reuters to be between the most 250 cited researchers in engineering in the world.